Published May 1, 1984

Endosome pH Measured in Single Cells by Dual Fluorescence Flow Cytometry: Rapid Acidification of Insulin to pH 6

ROBERT F. MURPHY,* SCOTT POWERS,‡ and CHARLES R. CANTOR*

Department of Human Genetics and Development and ‡Department of Biological Sciences, Columbia University, New York 10032. Dr. Murphy's present address is Department of Biological Sciences and Center for Fluorescence Research in Biomedical Sciences, Carnegie-Mellon University, Pittsburgh, Pennsylvania 15213. Dr. Powers' present address is Cold Spring Harbor Laboratory, Cold Spring Harbor, New York 11724.

ABSTRACT The acidification of various ligands was measured on a cell by cell basis for cell suspensions by correlated dual fluorescence flow cytometry. Mouse 3T3 cells were incubated with a mixture of fluorescein- and rhodamine-conjugated ligands, and the ratio of fluorescein and rhodamine fluorescence was used as a measure of endosome pH. The calibration of this ratio by both fluorometry and flow cytometry is described. Dual parameter histograms of average endosome pH per cell versus amount of internalization were calculated from this data, for samples in the absence and presence of chloroquine added to neutralize acidic cellular vesicles. The kinetics of acidification of insulin were measured and compared with previous results obtained with the chloroquine ratio technique. Rapid acidification of internalized ligand was observed both for insulin, which was mostly internalized via nonspecific pathways, and for α_2-macroglobulin, which was mainly internalized by specific receptor-mediated endocytosis. The average pH observed for internalized insulin was <pH 6 within 10 min after addition of insulin. At 30 min, the average pH began to decrease to ~pH 5, presumably because of fusion of endosomes with lysosomes.

The mechanism and kinetics of acidification of vesicles containing endocytosed material is of significant interest. This acidification has been proposed or demonstrated to play an important role in a variety of cellular processes (for review see reference 1). Gonzalez-Noriega et al. (2) proposed that the recycling of receptors for lysosomal enzymes required dissociation of ligand-receptor complexes at acidic pH. They demonstrated that this process could be inhibited by agents, such as chloroquine, that dissipate intravesicular pH gradients.

The cytoplasmic entry of many toxins and viruses is also facilitated by low pH. These include Semliki Forest virus (3, 4), diphtheria toxin (5, 6), and influenza virus (7, 8). Tetanus toxin fragment B has been shown to form channels in lipid vesicles at low pH (9). The effectiveness of these toxins and viruses is controlled by the competing processes of cytoplasmic entry and lysosomal degradation. Substances that raise the pH of acidic vesicles inhibit the toxicity of these agents by stopping both processes, while they enhance the toxicity of ricin (10), presumably by blocking only the latter (ricin has a pH optimum for toxicity close to neutrality).

The pH sensitivity of fluorescein fluorescence has been utilized to measure intracellular pH of cell suspensions in a standard fluorimeter (11), and of single cells by microspectrophotometry (12, 13) and flow cytometry (12). Ohkuma and Poole (14) pioneered the use of fluorescein-labeled probes to measure intravesicular pH in cell populations by fluorometry, using the ratio of fluorescein emission when excited by 495- and 450-nm light as an indicator of the pH of macrophage lysosomes containing endocytosed fluorescein isothiocyanate (FITC)[1]-conjugated dextran. This technique has been used to

[1] *Abbreviations used in this paper:* α_2-M, α_2-macroglobulin; FACS, fluorescence-activated cell sorter; FITC, RITC, and TRITC, fluorescein, rhodamine B, and tetramethyl-rhodamine isothiocyanate, respectively.

Published May 1, 1984

study the pH changes associated with phagolysosome formation (15) and the respiratory burst during phagocytosis (16).

We have previously reported rapid acidification of endocytic vesicles containing fluorescein-conjugated probes endocytosed after binding to the cell surface (17, 18). The flow cytometric method we developed uses measurements made both before and after the addition of a lysomotropic amine, such as chloroquine, to relieve the quenching of fluorescein contained in acidic vesicles. Rapid acidification was observed for molecules endocytosed by nonspecific adsorptive endocytosis (histone, reference 17) and by a combination of nonspecific and receptor-mediated endocytosis (insulin, reference 18). Similar rapid acidification has been observed by microspectrofluorimetry for α_2-macroglobulin (α_2-M) (19) and transferrin (20) in mouse fibroblasts, and for phagosomes of the ameba, *Chaos carolinensis* (21) and *Amoeba proteus* (22). In vitro acidification of endocytic vesicles has been demonstrated using FITC-dextran (23).

Since the previously reported methods require sequential measurements, they are unsuited for direct measurement of endosome pH in single cells by flow cytometry. Such direct measurements would be of great usefulness for analyzing possible heterogeneity in endosome acidification from cell to cell, and for the isolation of acidification variants by flow sorting. In this report we describe the use of dual fluorescence flow cytometry to obtain statistically significant measurements of the kinetics of acidification of endocytic vesicles.

MATERIALS AND METHODS

Reagents and Cell Culture: All reagents were obtained from Sigma Chemical Co. (St. Louis, MO) unless otherwise specified. Bovine pancreatic insulin was labeled with FITC, rhodamine B isothiocyanate (RITC) and tetramethyl-rhodamine isothiocyanate (TRITC, Research Organics, Inc., Cleveland, OH) on lysine residue B29 as described previously (18). FITC- and TRITC-labeled α_2-M were the gifts of Dr. F. Maxfield (New York University).

Mouse Swiss 3T3 fibroblasts were grown in monolayer cultures in Dulbecco's modified Eagle's medium supplemented with 10% fetal calf serum (Gibco Laboratories, Grand Island, NY), 100 U/ml penicillin, and 100 μg/ml streptomycin sulfate. Probes were added directly to the medium of subconfluent monolayers 2 d after plating and cells were harvested by trypsinization (18). The trypsinization protocol removes uninternalized, surface-bound probe, since no cell-associated FITC fluorescence was detected for cells incubated with FITC-insulin on ice and then trypsinized (18). Samples were analyzed by flow cytometry at room temperature immediately after trypsinization. Since vesicle fusion has been reported to be inhibited below 24°C (24), acidification kinetics measured by this protocol should be accurate to within the 10-min trypsinization period.

Flow Cytometry: A fluorescence-activated cell sorter (FACS IV, Becton Dickinson FACS Systems, Sunnyvale, CA) interfaced with a VAX 11/780 computer (Digital Equipment Corp., Maynard, MA) was used for all analyses. For all dual fluorescence histograms, a forward angle light-scattering gate was used to eliminate dead and clumped cells. Sample temperature was maintained with a circulating water bath. Optical filters were obtained from Ditric Optics (Hudson, MA). 2.02 μm-diam beads were obtained from Becton Dickinson.

For the experiments shown in Figs. 2 and 3, excitation was with 496.5-nm line of an argon ion laser (200 mol wt). A 520-nm long-pass dielectric filter (520LP) and a 530-nm long-pass glass filter (530LP) were placed in the filter holder before the 50% beam splitter. Green fluorescence was measured using an 540-nm short-pass filter (540SP) and a 9524A photomultiplier tube with a high voltage of 700 V. Red fluorescence was measured with a 580-nm long-pass dielectric filter (580LP) and a 600-nm long-pass epoxy filter (600LP), and 9798B photomultiplier tube with a high voltage of 850 V. An analog dual fluorescence compensation network (25) was used to subtract 13% of the green signal from the red signal. The data in Fig. 4 and 5 were obtained similarly, with the following changes: Fig. 4, no analog dual fluorescence compensation; Fig. 5, the 580LP was eliminated and 17% compensation was used.

Conversion of Fluorescein/Rhodamine B Ratio to pH: Fluorescence emission spectra were recorded with either 458- or 497-nm excitation using a Schoeffel RRS1000 fluorimeter under the control of a Tektronix model 31 calculator (Tektronix, Inc., Beaverton, OR), and transferred directly to the VAX 11/780. The transmission spectra of the combined 520LP, 530LP, and 540SP and the combined 520LP, 530LP, and 620LP used for the FACS experiments were also entered into the VAX. The product of the fluorescence intensity at each wavelength and the transmission of the appropriate filter set at that wavelength were calculated, and the resulting curve was then integrated to give total fluorescence intensity that would be expected to pass through the filter (Fig. 1*A*).

RESULTS

pH Sensitivities of Fluorescein and Rhodamine

All fluorescence methods of determining pH use a ratio of two separate measurements, for example fluorescein emission at two excitation wavelengths (14) or quenched and unquenched fluorescence emission (17, 18). The possibility of pH measurements using dual excitation and flow cytometry has been suggested (12), but the use of this method has not been reported. We investigated the possibility of using two

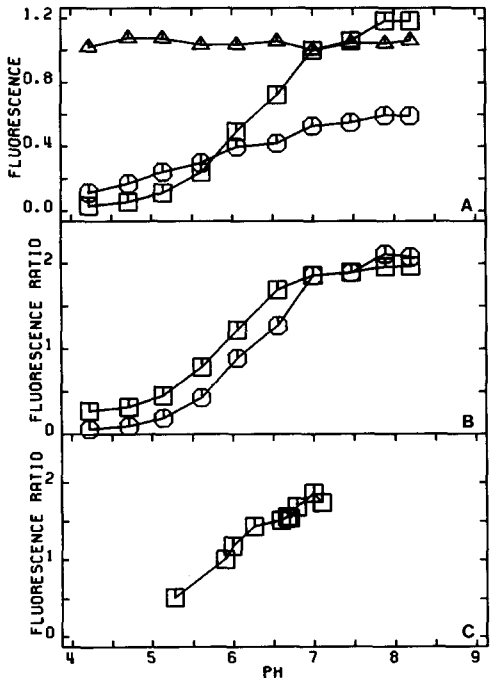

FIGURE 1 pH dependence of fluorescein and rhodamine B fluorescence under flow cytometric conditions. (*A*) 0.14 μM solutions of either fluorescein (□, ○) or rhodamine B (△) were prepared in PBS at various pHs. Fluorescence emission spectra were recorded with excitation at either 458 nm (○) or 297 nm (□, △) and convoluted with the filter characteristics as described in Materials and Methods. The values for fluorescein are in arbitrary units and those for rhodamine B have been normalized to equal the emission of fluorescein with 497-nm excitation at pH 7.0. (*B*) The ratio of the fluorescein fluorescence with 497-nm excitation to that with 458-nm excitation (□), and the ratio of fluorescein fluorescence with 497-nm excitation to the rhodamine fluorescence (○), was calculated for each pH value from the data in *A*. (*C*) A similar calibration curve was created using the FACS. Equal concentrations of FITC- and TRITC-insulin were added to solutions containing 2.02-μm beads in PBS at different pHs. The presence of the free fluorochromes in the volume surrounding each bead as it passes through the laser beam causes a detectable increase in the red and green fluorescence. Dual parameter histograms were recorded for these samples and the ratio of the mean green and red fluorescence (after subtraction of the mean fluorescence of a bead in PBS alone) was calculated for the singlet bead peak (□).

Published May 1, 1984

fluorescent probes, one pH sensitive (fluorescein derivatives) and one pH insensitive (rhodamine derivatives), excited by the same wavelength. The significant overlap in emission spectra of these dyes is the major problem with this approach. Loken, Parks, and Herzenberg (25) have described single laser excitation of fluorescein and tetramethyl rhodamine conjugates using the 514.5-nm argon ion laser line. Under these conditions, there is minimal spillover of fluorescein emission into the rhodamine channel, but appreciable spillover of rhodamine into the fluorescein channel. These authors described an electronic cross-coupling system which they used to eliminate this spillover.

Since for our purposes the fluorescein signal was to provide an indication of pH while the rhodamine signal was used as a measure of total internalization, minimal spillover of rhodamine to fluorescein was desirable. In addition, the excitation at 514.5 nm makes it difficult to eliminate scattered laser light from the fluorescein channel, especially for large cells such as fibroblasts. We therefore have used excitation at 496.5 nm, along with appropriate optical filters.

The pH sensitivity of both dyes under these conditions is shown in Fig. 1*A*. While fluorescein fluorescence is strongly pH dependent at both excitation wavelengths, the lower slope of the 458-nm excitation curve causes the F497/F458 ratio to vary with pH. In contrast, rhodamine fluorescence is unaffected by pH over the range 4–8.5, and as one might expect, the sensitivity of the fluorescein/rhodamine ratio is even greater (Fig. 1*B*). This curve can be used to calculate pH values from observed fluorescein/rhodamine ratios, once these ratios have been corrected for autofluorescence and spillover, as discussed below. Fig. 1*C* shows the results of direct calibration by flow cytometry using 2.02-μm beads in dilute solutions of the two probes with various pH values. The presence of the probes in the small volume surrounding the bead during its passage through the laser produces fluorescent signals that can be used to determine the detection efficiencies of the two dyes and to measure the FITC/TRITC ratio at various pH values. The calibration curve in Fig. 1*C* is similar to that in Fig. 1*B*, but is slightly shifted towards low pH. Such a difference between predicted and observed pH calibration curves has been described previously (13); in our case it may be due to some equilibration of the sample with the sheath fluid (pH 7.3) during the few microseconds they are in contact before the measurement.

Measurement of Endosome pH in Single Cells

Swiss 3T3 cell monolayers were incubated with FITC- and/or RITC-insulin for various periods of time, trypsinized, and analyzed by flow cytometry. Dual parameter histograms for cells incubated for 30 min are shown in Fig. 2. The addition of chloroquine to neutralize acidic vesicles clearly demonstrates the quenching of FITC (Fig. 2, *B* and *D*) but not RITC (Fig. 2, *C* and *D*). 1–2% of the cells are found in the triangular region to the right of the main cluster in Fig. 2*D*, indicating that some cells have failed to acidify the internalized insulin.

The data of Fig. 2 were collected using analog dual fluorescence compensation to eliminate spillover of FITC fluorescence into the RITC channel. However, Fig. 2 shows that apparent spillover of RITC fluorescence into the FITC channel also occurred. Most of this is due to broad spectrum autofluorescence (Fig. 2*A*). The RITC-FITC spillover can be eliminated digitally, as shown in Fig. 3*A* for the data of Fig. 2*D*. The change resulting from chloroquine addition may be

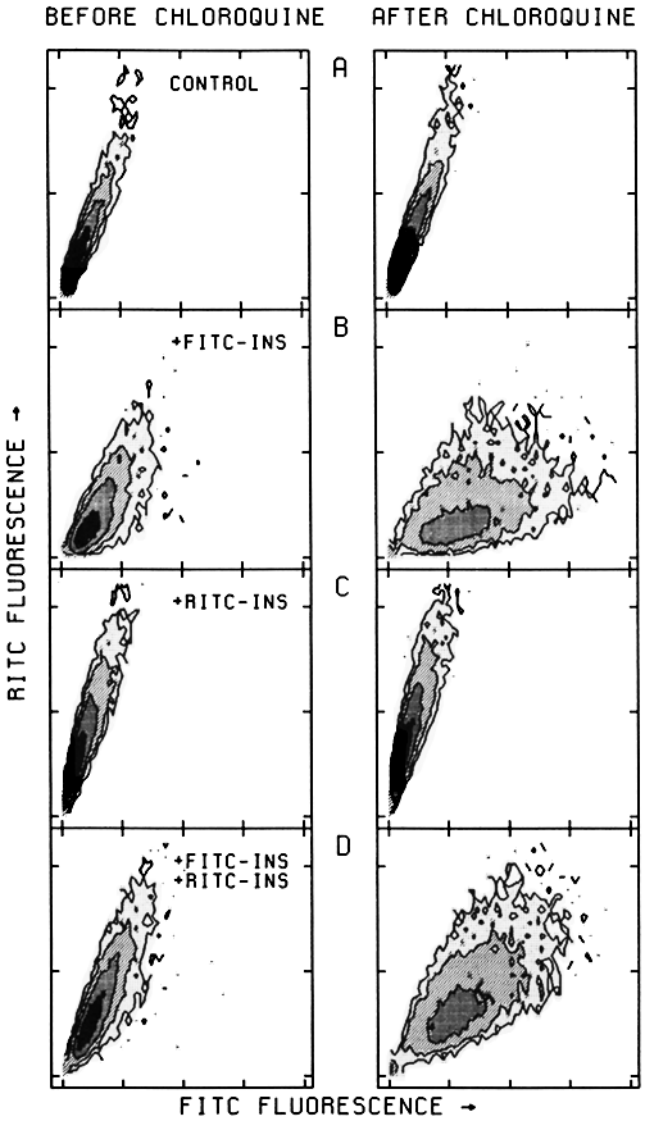

FIGURE 2 Acidification of insulin by 3T3 cells. Monolayers were incubated with no addition (*A*), 1 μM FITC-insulin (*B*), 1 μM RITC-insulin (*C*), or both 1 μM FITC-insulin and 1 μM RITC-insulin (*D*) for 30 min at 37°C and then trypsinized and analyzed as described in Materials and Methods (*left*). After analysis, the remaining sample was analyzed 30 min after the addition of 100 μM chloroquine (*right*). Histograms of 10,000 cells were obtained with the same machine settings for all samples. The contours are drawn at 2, 8, 32, and 128 cells and the axes are marked every 16 channels. Note the presence of cells in the non-chloroquine-treated samples that have not acidified the labeled insulin (those to the right of the main peak in *B* and *D*).

clearly seen, and it is also reflected in the ratio of the RITC and FITC signals (Fig. 3*B*). Using the calibration curve of FITC/RITC ratio versus pH (Fig. 1*B*), we can express the results as pH versus amount of internalization (Fig. 3, *C* and *D*). This can be done by either of two methods. The autofluorescence and spillover can be subtracted before calculating the FITC/RITC ratio and interpolating using Fig. 1, in which case inaccurate (and in some cases undefined) values will be obtained for cells with FITC or RITC values close to autofluorescence (Fig. 3*C*). Alternatively, a new calibration curve can be obtained by adding the average autofluorescence for each fluor to the FITC and RITC measurements of Fig. 1*A* before calculating their ratio. This curve can then be com-

Published May 1, 1984

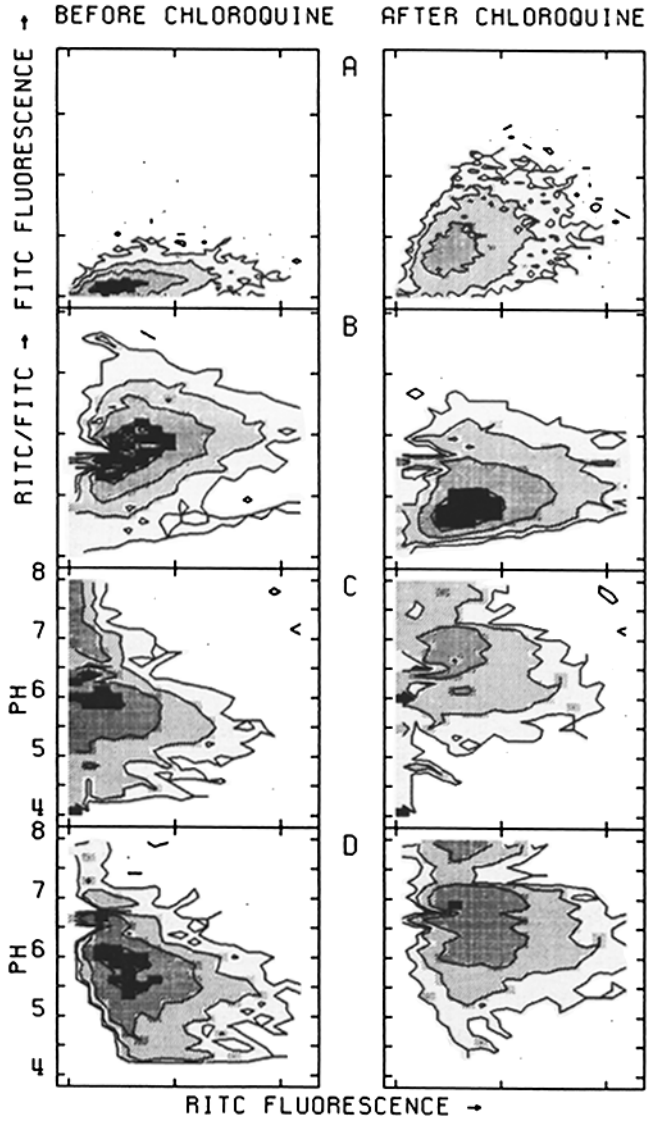

FIGURE 3 Conversion of fluorescence measurements to vesicle pH. (*A*) The data of Fig. 3*D* after correction for 48% spillover of RITC fluorescence into the FITC detector. (*B*) Average RITC/FITC ratio (without spillover correction) for each cell versus RITC fluorescence (C) Average vesicle pH for each cell versus RITC fluorescence. Contours are drawn at 2, 8, 32, and 128 cells. The average calculated pHs for C and *D* are 5.7 ± 1.0 and 5.6 ± 0.6 for the non-chloroquine-treated sample and 6.3 ± 1.1 and 6.5 ± 0.9 for the chloroquine-treated sample.

pared with the FITC/RITC ratio of each cell with spillover correction but without background subtraction (Fig. 3*D*). The later method is preferable when the autofluorescence is in the range of 5–20% of the maximal corrected fluorescence for each fluor. When autofluorescence and spillover are minimized, either by the use of fluorochromes with better separation of emissions or by the use of dual wavelength excitation, both methods should yield comparable results.

Fig. 3 clearly demonstrates the feasibility of making vesicle pH measurements on large numbers of single cells by flow cytometry. The operations necessary for the pH calculation for a 64 by 64 channel histogram take <5 s on a VAX 11/780. In the absence of high speed computer capability, a simple analog circuit to perform this pH calculation can be added to existing flow cytometers.

The kinetics of acidification of insulin by 3T3 cells measured by this approach is shown in Fig. 4. By 10 min, the RITC/FITC ratio is already lower than that for chloroquine-treated cells, indicating that some acidification has occurred by this time. McNeil et al. have observed a similar decrease in pH beginning immediately after binding of FITC-ribonuclease to the surface of ameba (22). The FITC/RITC ratio remains fairly constant during the first 20 min at a pH just below 6, and then decreases starting at 30 min and continuing through 2 h. This transition at 30 min agrees well with our earlier observation of a peak in the ratio of FITC-insulin fluorescence with and without chloroquine addition (18). A difference between these previous results and the data of Fig. 4 is worth noting. The chloroquine ratio increased to 30 min and then decreased slightly. A similar peak followed by a slow decline at longer times was observed for histone (17). The FITC/RITC ratio continues to decrease after 30 min (Fig. 4). It is probable that the later decrease in the chloroquine experiments is the result of incomplete neutralization by chloroquine of the strongly acidic compartments (presumably lysosomes) encountered at later times, and complete neutralization of the mildly acidic compartments at early times. Such an incomplete neutralization by chloroquine was observed by Ohkuma and Poole (14) for macrophage lysosomes containing FITC-dextran.

Under the conditions of these experiments, insulin endocytosis occurs via both specific and nonspecific mechanisms. The endocytosis of histone follows rapid, nonspecific binding to the cell membrane. Both molecules are rapidly acidified after endocytosis. Fig. 5 shows that the serum protein α_2-M is also acidified within 30 min, confirming by a different method the initial report of Tycko and Maxfield (19). Since the internalization of α_2-M is >92% specific (Fig. 5, *C* and *D*), this acidification step is common to both specific and nonspecific adsorptive endocytosis.

DISCUSSION

Flow Cytometric Measurement of Vesicle pH

The dual fluorescence flow cytometric method that we have described has a number of advantages for the study of endo-

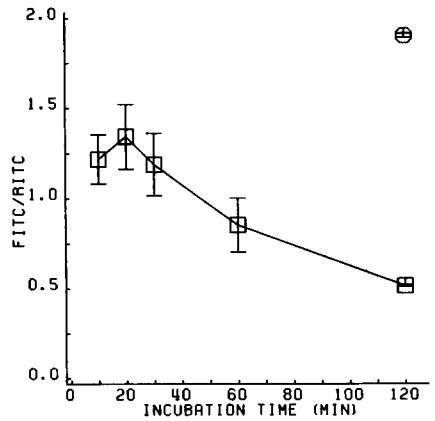

FIGURE 4 Kinetics of acidification of insulin. 3T3 monolayers were incubated with 0.5 μM each of FITC-insulin and RITC-insulin for various periods of time and then analyzed as described in Materials and Methods. The average ratio of the FITC and RITC fluorescence per cell was calculated for duplicate samples (□). After analysis, the 120-min samples were treated with chloroquine and reanalyzed (○). The error bars represent ± 1 SD.

Published May 1, 1984

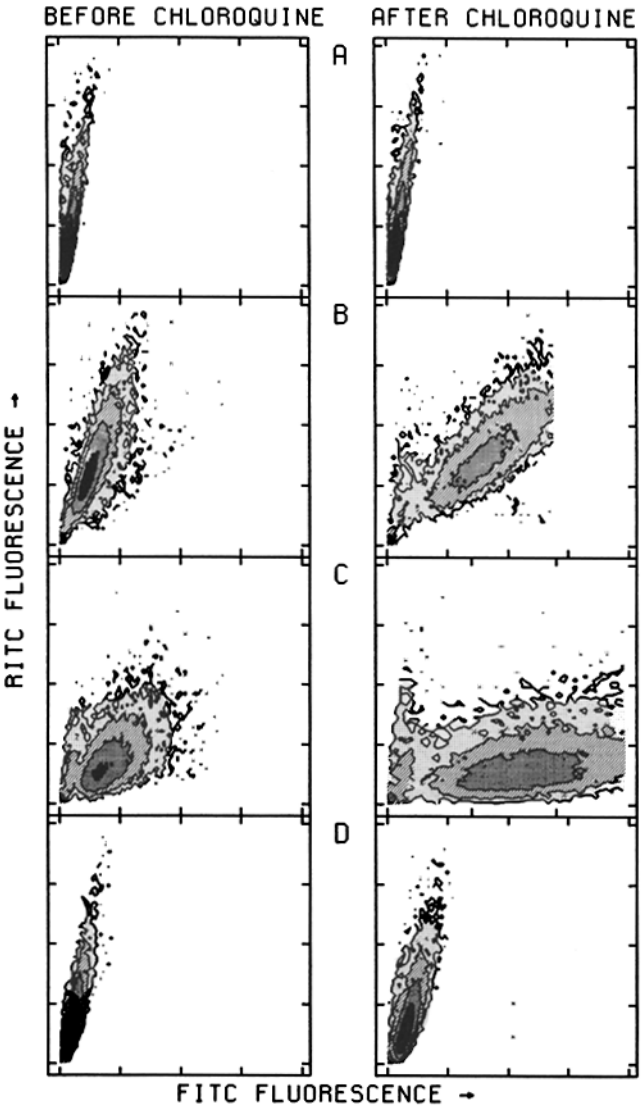

FIGURE 5 Acidification of specifically endocytosed α_2-M. 3T3 monolayers were washed twice with serum-free medium and then incubated at 37°C for 30 min with no addition (*A*), 80 μg/ml each of FITC-α_2-M and RITC-α_2-M (*B*), 80 μg/ml FITC-α_2-M alone (*C*), or 80 μg/ml FITC-α_2-M and 3 mg/ml unlabeled α_2-M (*D*). All histograms (20,000 cells) were obtained with the same machine settings, with the exception of *C* (*right*) which was recorded with the FITC fluorescence gain reduced by one-half (the figure has been normalized accordingly). Contours are drawn at 2, 8, 32, and 128 cells. Calculation of the mean FITC fluorescence for the chloroquine-treated samples in *C* and *D* yields a value of 92% for the amount of specific α_2-M endocytosis.

some acidification and processing. First, many cells can be measured for each histogram, in a single time course. Second, the cells not being measured can be maintained at any desired temperature by a circulating water bath connected to the jacketed sample holder. Third, dead or dying cells can be excluded from analysis by light scattering or fluorescence criteria. Lastly, since each cell is exposed to exciting light only once and for a brief time, photobleaching and photolysis, which may cause problems during continuous microscopic observation of a single cell, are essentially eliminated. However, while cells may be analyzed while attached to microspheres or other carriers (26), little or no spatial information is obtained. Thus, flow cytometry may be used to provide statistically significant quantitation and kinetic analysis while fluorescence microscopy is used to provide spatial information on adherent cells.

Given the importance of vesicle acidification for receptor recycling and toxin and virus action, the method we have described should be an important tool for extending our knowledge of the role of vesicle acidification in cellular processes. For example, we have used this method to demonstrate that mouse histocompatibility antigens are acidified by activated T lymphocytes (27). Flow sorting of cells that show diminished or enhanced vesicle acidification may be used to establish variant cell lines and thereby provide information regarding the genetic control of vesicle and lysosome acidification. Flow cytometric analysis may also have potential clinical importance for early detection of abnormal ligand acidification. It should be pointed out that the fluorescein-rhodamine ratio method is not limited to analysis of endocytosed material. For example, changes in cytoplasmic pH may be measured using a mixture of fluorescein- and rhodamine-conjugated dextrans introduced into the cytoplasm by one of the variety of cell loading techniques.

Acidification and Lysosomal Fusion

Rapid acidification of molecules endocytosed adsorptively has now been demonstrated for a number of ligands and cell systems (17–19, 21). The ratio excitation method of Ohkuma and Poole (14) has been used to demonstrate that α_2-M is contained in acidic vesicles after a 15-min incubation and a 5-min chase (19). We have confirmed these results by dual label flow cytometry (Fig. 5).

We have previously reported that chloroquine produces a much smaller increase in the fluorescence of FITC-dextran than that of FITC-insulin, for samples incubated with probe for from 10 min to 3 h (18). This might be interpreted as an indication that fluid pinosomes are acidified less rapidly or to a lesser extent than adsorptive pinosomes. However, we interpret the previous results to be due to the abnormal fluorescence properties of FITC-dextran in the presence of chloroquine (14). Isolated endosomes and/or lysosomes containing FITC-dextran have been shown to be capable of acidifying their contents in vitro (23).

The results obtained in Fig. 4 provide evidence that endosome acidification occurs very rapidly after internalization and that the endosome pH remains slightly below pH 6 for ~30 min. After this work was completed, biphasic acidification kinetics were reported for a Chinese hamster ovary K1 mutant cell line (28). The difference in lysosomal fusion time between the results of Merion et al. (15–20 min) and the results of Fig. 4 (30 min) may also be due to the differences in probe and cell type in the two experiments. However, the differences may be due to possible effects of trypsin internalized during removal of the cells before analysis. Future experiments using a different removal technique (such as collagenase) or with cells on microspheres will be needed to resolve this question.

As discussed above, we interpret the decrease in pH occurring after 30 min to result from lysosomal fusion. Tycko and Maxfield (19) have presented micrographs of 3T3 cells incubated with rhodamine-conjugated α_2-M for a total of 20 min before fixation and staining for acid phosphatase. They stated that no overlap between rhodamine-α_2-M and acid phosphatase activity was observed, although some overlap is evident

Published May 1, 1984

in the published micrographs. We have performed extensive analysis of fibroblasts incubated with FITC- or TRITC-insulin for periods from 5 to 60 min and then stained for acid phosphatase after fixation (data not shown). We have concluded that comparison of bright field and fluorescent images is insufficient to resolve questions regarding presence or absence of a ligand in lysosomes, since (*a*) significant numbers of dark "lysosomes" are seen in control cells not stained for acid phosphatase (as an example see Fig. 2 *f* in reference 29) making acid phosphatase staining patterns difficult to interpret; (*b*) alignment of individual vesicles is subject to significant error owing to focusing errors and sample movement; and (*c*) collection of statistically significant data is difficult. The frequently stated observation that lysosomes are predominantly distributed around the nucleus while primary endocytic vesicles and endosomes are in the cell periphery suggests that acidification is taking place before lysosomal fusion. However, published micrographs of internalized α_2-M after a 20-min incubation (conditions under which the average pH was measured as pH 5.0) show perinuclear staining suggestive of lysosomes (Fig. 2 of reference 22). While most direct (fluorescence) and indirect (virus fusion) data is consistent with acidification to ~pH 6 soon after endocytic vesicle formation, the determination of whether further acidification takes place only through lysosomal fusion must await further technical developments, such as the synthesis of fluorogenic substrates for lysosomal enzymes which can be covalently attached to ligands.

We thank Mr. K. Yamamoto for technical assistance, Dr. F. Maxfield for the gift of α_2-M, and Dr. R. Pollack for providing cell culture facilities. We also thank Drs. E. Holtzman, F. Maxfield, P. McNeil, and D. L. Taylor for helpful discussions.

This work was supported in part by postdoctoral fellowship DRG-352-F from the Damon Runyon-Walter Winchell Cancer Foundation (to R. F. Murphy) and by NIH grant GM-27576 (to C. R. Cantor).

Received for publication 26 October 1983, and in revised form 27 January 1984.

REFERENCES

1. Steinman, R. M., I. S. Mellman, W. A. Muller, and Z. A. Cohn. 1983. Endocytosis and the recycling of plasma membrane. *J. Cell Biol.* 96:1–27.
2. Gonzalez-Noriega, A., J. H. Grubb, V. Talkad, and W. S. Sly. 1980. Chloroquine inhibits lysosomal enzyme pinocytosis and enhances lysosomal enzyme secretion by impairing receptor recycling. *J. Cell Biol.* 85:839–852.
3. Helenius, A., J. Kartenbeck, K. Simons, and E. Fries. 1980. On the entry of Semliki Forest virus into BHK-21 cells. *J. Cell Biol.* 84:404–420.
4. Marsh, M., E. Bolzau, and A. Helenius. 1983. Penetration of semliki forest virus from acidic prelysosomal vacuoles. *Cell.* 32:931–940.
5. Sandvig, K., and S. Olsnes. 1980. Diptheria toxin entry into cells is facilitated by low pH. *J. Cell Biol.* 87:828–832.
6. Draper, R. K., and M. I. Simon. 1980. The entry of diptheria toxin into the mammalian cell cytoplasm: evidence for lysosomal involvement. *J. Cell Biol.* 87:849–854.
7. Matlin, K. S., H. Reggio, A. Helenius, and K. Simons. 1981. Infectious entry pathway of infuenza virus in a canine kidney cell line. *J. Cell Biol.* 91:601–613.
8. Yoshimura, A., K. Kuroda, K. Kawasaki, S. Yamashina, T. Maeda, and S.-I. Ohnishi. 1982. Infectious cell entry mechanism of influenza virus. *J. Virol.* 43:284–293.
9. Boquet, P., and E. Duflot. 1982. Tetanus toxin fragment forms channels in lipid vesicles at low pH. *Proc. Natl. Acad. Sci. USA.* 79:7614–7618.
10. Ray, B., and H. C. Wu. 1981. Enhancement of cytotoxicities of ricin and Pseudomonas toxin in Chinese hamster ovary cells by nigericin. *Mol. Cell Biol.* 1:552–559.
11. Thomas, J. A., R. N. Buchsbaum, A. Zimniak, and E. Racker. 1979. Intracellular pH measurements in Ehrlich ascites tumor cells utilizing spectroscopic probes generated in situ. *Biochemistry.* 18:2210–2218.
12. Visser, J. W. M., A. A. M. Jongeling, and H. J. Tanke. 1979. Intracellular pH-determination by fluorescence measurements. *J. Histochem. Cytochem.* 27:32–35.
13. Heiple, J. M., and D. L. Taylor. 1980. Intracellular pH in single motile cells. *J. Cell Biol.* 86:885–890.
14. Ohkuma, S., and B. Poole. 1978. Fluorescence probe measurement of the intralysosomal pH in living cells and the perturbation of pH by various agents. *Proc. Natl. Acad. Sci. USA.* 75:3327–3331.
15. Geisow, M. J., P. D'Arcy Hart, and M. R. Young. 1981. Temporal changes of lysosome and phagosome pH during phagolysosome formation in macrophages. *J. Cell Biol.* 89:645–652.
16. Segal, A. W., M. Geisow, R. Garcia, A. Harper, and R. Miller. 1981. The respiratory burst of phagocytic cells is associated with a rise in vacuolar pH. *Nature (Lond.).* 290:406–409.
17. Murphy, R. F., E. D. Jorgensen, and C. R. Cantor. 1982. Kinetics of histone endocytosis in Chinese hamster ovary cells. A flow cytofluorometric analysis. *J. Biol. Chem.* 257:1695–1701.
18. Murphy, R. F., S. Powers, M. Verderame, C. R. Cantor, and R. Pollack. 1982. Flow cytofluorometric analysis of insulin binding and internalization by Swiss 3T3 cells. *Cytometry.* 2:402–406.
19. Tycko, B., and F. R. Maxfield. 1982. Rapid acidification of endocytic vesicles containing α_2-macroglobulin. *Cell.* 28:643–651.
20. Van Renswoude, J., K. R. Bridges, J. B. Harford, and R. D. Klausner. 1982. Receptor-mediated endocytosis of transferrin and the uptake of Fe in K562 cells: identification of a nonlysosomal acidic compartment. *Proc. Natl. Acad. Sci. USA.* 79:6186–6190.
21. Heiple, J. M., and D. L. Taylor. 1982. pH changes in pinosomes and phagosomes in the ameba, Chaos carolinensis. *J. Cell Biol.* 94:143–149.
22. McNeil, P. L., L. Tanasugarn, J. B. Meigs, and D. L. Taylor. 1983. Acidification of phagosomes is initiated before lysosomal enzyme activity is detected. *J. Cell Biol.* 97:692–702.
23. Galloway, C. J., G. E. Dean, M. Marsh, G. Rudnick, and I. Mellman. 1983. Acidification of macrophage and fibroblast endocytic vesicles in vitro. *Proc. Natl. Acad. Sci. USA.* 80:3334–3338.
24. Oka, J. A., and P. H. Weigel. 1983. Recycling of the asialoglycoprotein receptor in isolated rat hepatocytes. *J. Biol. Chem.* 258:10253–10262.
25. Loken, M. R., D. R. Parks, and L. A. Herzenberg. 1977. Two-color immunofluorescence using a fluorescence-activated cell sorter. *J. Histochem. Cytochem.* 25:899–907.
26. Bloch, D. B., B. R. Smith, and K. A. Ault. 1983. Cells on microspheres: a new technique for flow cytometric analysis of adherent cells. *Cytometry.* 3:449–452.
27. Murphy, R. F., D. B. Tse, C. R. Cantor, and B. Pernis. 1984. Acidification of internalized class I MHC antigen by T lymphoblasts. *Cell. Immunol. In press.*
28. Merion, M., P. Schlesinger, R. M. Brooks, J. M. Moehring, T. J. Moehring, and W. S. Sly. 1983. Defective acidification of endosomes in Chinese hamster ovary cell mutants "cross-resistant" to toxins and viruses. *Proc. Natl. Acad. Sci. USA.* 80:5315–5319.
29. Yamashiro, D. J., S. R. Fluss, and F. R. Maxfield. 1983. Acidification of endocytic vesicles by an ATP-dependent proton pump. *J. Cell Biol.* 97:929–934.